

INFRARED MICROSPECTROSCOPY TO INVESTIGATE STRUCTURAL CHANGES OF SUBCHONDRAL BONE AND ARTICULAR CARTILAGE IN OSTEOARTHRITIC KNEE

Kanjana Thumanu¹, Duangjai Srisamut¹, Apichart Ngernsoungnern², Piyada Ngernsoungnern², Supatcharee Siriwong², Anucha Chomnonloa², Piyachart Songvijit², Chotima Poompramun³, and Bura Sindhupakorn^{4*}

Received: October 24, 2017; Revised: November 28, 2017; Accepted: November 29, 2017

Abstract

Osteoarthritis (OA) is characterized by degeneration of the articular cartilage and thickening of the subchondral bone. The aim of this study is to investigate the changing of the biochemical components of the cartilage and bone in OA of the knee by using histochemical staining and synchrotron infrared microspectroscopy (SR-IR). Three samples were collected from the medial and lateral condyle of the femur. The control group is 21 years old and 47 and 82 years old are the ages of the experimental groups. Histochemical staining was done with hematoxylin and eosin stain, alcian blue. Regarding the results in the articular cartilage, the peak intensities of amide I significantly decreased (0.2073 ± 0.0019 and 0.2070 ± 0.00270) in the 47 years old and 82 years old OA knees, respectively, when compared to the normal 21 years old (0.2154 ± 0.0009). The subchondral bone of both (0.2133 ± 0.0008 and 0.2122 ± 0.0007 , respectively) were significantly higher than the normal (0.2084 ± 0.0009). Amide II significantly decreased in the 82 years old (0.0936 ± 0.0054) compared to the 47 years old (0.1057 ± 0.0013), but was still at a higher level than the normal (0.0854 ± 0.0016). The peak intensity of amide II in the calcified cartilages was not different in all the knees. The peak intensity of proteoglycans was

¹ Synchrotron Light Research Institute (Public Organization), Nakhon Ratchasima 30000, Thailand. E-mail: kthumanu@gmail.com; duangjai@slri.or.th

² School of Preclinic, Institute of Science, Suranaree University of Technology, Nakhon Ratchasima, 30000, Thailand. E-mail: apichart@sut.ac.th; npiyada@sut.ac.th; supatcharee5010424@gmail.com; armter_man@hotmail.com; kik0505@hotmail.com

³ School of Animal Production Technology, Suranaree University of Technology, Nakhon Ratchasima, 30000, Thailand. E-mail: cp.chotima@gmail.com

⁴ Orthopedic Department, Medical Faculty, Institute of Medicine, Suranaree University of Technology, Nakhon Ratchasima, 30000, Thailand. E-mail: bura@sut.ac.th; Tel.: 080-5886686

* Corresponding author

significantly highest in the articular cartilage of the 47 years old (0.0377 ± 0.0045). Cartilage was the main structure that was affected by decreases in the level of amides in the OA. OA also was involved in a change in the orientation of the collagen fibrils and structure. This study demonstrated that SR-IR can rapidly characterize the distribution and structure of changes in the cartilage.

Keywords: Infrared microspectroscopy, osteoarthritis, articular cartilage

Introduction

Osteoarthritis (OA) is an aging disease in which mechanical factors have an important role. This disease is characterized by the degenerative articular cartilage (AC) and thickening of the subchondral bone (SB) under the cartilage (Radin *et al.*, 1970; Kamibayashi *et al.*, 1995). Under normal conditions, the pressure load is transmitted through the joints by the AC and SB. Therefore, the SB density and cartilage thickness are required for an adequate function (Eckstein *et al.*, 1992; Eckstein *et al.*, 1998). The changes in the density and the architecture of the SB have a tremendous effect on both the initiation and progression of cartilage degeneration. Sindhupakorn *et al.* (2017) investigated structural changes in the periarticular bone which occurred in the development of OA using induced X-ray fluorescence analysis, X-ray absorption near edge structure, and the extended X-ray absorption fine structure technique at the Ca K-edge. The degenerated changes in calcium structures were identified when the age was increased. Cortical and trabecular bones rapidly altered the skeletal architecture and shape which may be related to the differential capacity of the cartilage and bone to adapt to mechanical loads and damage (Goldring and Goldring, 2010). Many studies, such as gene, radiological, histological, and histochemical studies have tried to identify changes in human OA (Muller-Gerbl *et al.*, 1989; Eckstein *et al.*, 1995; Matsui *et al.*, 1997; Bobinac *et al.*, 2003; Lajeunesse, 2004; Aigner *et al.*, 2006; Ijiri *et al.*, 2008). Fourier transform infrared spectroscopy (FTIR) was used to map region-dependent changes in collagen, proteoglycans, and mineral distribution (Chappard *et al.*, 2006). The FTIR

technique combined with multivariate data analysis can be applied to study quantitative and qualitative changes of human AC by monitoring composition changes that occur with OA progression related to the content of amide I and carbohydrate. The disorder coil collagen increases significantly during the early progression of OA. The main structural components of AC such as collagen and proteoglycans of immature, mature, and degenerative cartilage can be studied by using FTIR microspectroscopy combined with multivariate data analysis. It was found that the significant degradation of amide I collagen was found in the advanced stage of OA (Saarakkala *et al.*, 2003; Khanarian *et al.*, 2014).

Some studies have reported that degradation and destruction of the femoral AC had a greater degree of deterioration than those of the tibial- and patellar-articular cartilage in patients with early stages of OA of the knee (Hada *et al.*, 2014). A study of the correlation between AC degeneration and bone morphometric parameters in OA knees revealed that degeneration of joint cartilage was generally more severe in the medial femoral condyle than that in the lateral one (Temple *et al.*, 2007). The aim of the present study was to investigate the changes in the biochemical components of the cartilage and underlying SB of the medial condyle of the femur in a comparison between normal and OA knees. We combined both the SR-IR microspectroscopy technique and histochemical staining in order to investigate changes in the biochemical components of the samples concerning differences in the materials present - protein amide I, II, and III, and proteoglycans.

Materials and Methods

Sample Isolation: Collection of Bone and Cartilage from the Medial Condyle of the Femur

Medial condyles of the femur were collected from males and females. The studied OA knees were collected from patients who were 47 years old (young OA) and 82 years old (aged OA) who underwent total knee arthroplasty. The studied subjects were graded for OA by the Kellgren and Lawrence system in grade 3 (Kellgren and Lawrence, 2000). The control samples were collected from a patient (21 years old) who underwent anterior cruciate ligament reconstruction with notchplasty and had no macroscopic evidence of AC degeneration or osteoarthritis. Exclusion criteria included patients who had an inflammatory joint disease, steroid injection prior to surgery, high blood calcium, and current drug history of mmbisphosphonate therapy. Tissue samples were collected using a cylindrical osteochondral explant with the approval of the medical ethics commission, consent of the medical institute of Suranaree University of Technology, and consent on the patient form. The sizes of the samples were 3-4 cm × 0.5 cm.

Tissue Preparation

All samples were fixed with 10% neutral buffered formalin (Sigma-Aldrich, St. Louis, MO, USA), followed by washing with 70% ethanol. Decalcification was performed by submerging the tissues in Decalcifying Solution-Lite (Sigma-Aldrich). The tissues were subsequently dehydrated, embedded in paraffin, and then sectioned at 5 μm thick. After deparaffinization and rehydration, the sections were stained with: 1) Mayer's hematoxylin and eosin (Bio-Optica, Milan, Italy) for the conventional histological study; 2) alcian blue pH 2.5 (Sigma-Aldrich) for studying the presence of proteoglycans; and 3) Masson's trichrome (Abcam, Cambridge, UK) for identifying the collagen fibers and bone matrix (Schmitz *et al.*, 2010). Finally, all stained sections were dehydrated, cleared,

mounted, and observed under a light microscope (80i, Nikon, Tokyo, Japan). The photographs were captured with a digital camera (BP72, Olympus, Tokyo, Japan).

SR-IR Microspectroscopy

Spectra data were collected at an infrared microspectroscopy beamline (BL4.1 IR Spectroscopy and Imaging) at the Synchrotron Light Research Institute (SLRI). Spectra were acquired with a Vertex 70 FTIR spectrometer (Bruker Optics, Ettlingen, Germany) coupled with an IR microscope (Hyperion 2000, Bruker) with a mercury cadmium telluride detector cooled with liquid nitrogen over the measurement range from 4000 to 800 cm⁻¹. The microscope was connected to a software-controlled microscope stage and placed in a specially designed box that was purged with dry air. The measurements were performed using an aperture size of 10×10 μm with a spectral resolution of 4 cm⁻¹, with 64 scans co-added. Spectral acquisition and instrument control was performed using OPUS 7.2 (Bruker Optics Ltd, Ettlingen, Germany) software. The spectral changes of the functional groups were performed at the integral area of each peak, especially the region of amide I collagen (1700-1600 cm⁻¹), amide II collagen (1600-1500 cm⁻¹), amide III collagen (1338 cm⁻¹), and proteoglycan carbohydrate (1140-985 cm⁻¹).

Statistical Analysis

The spectra from each component of the subchondral bone and articular cartilage sample were baseline correct, using 9 smoothing points, and vector normalized by the Savitzky-Golay method (3rd polynomial, 13 smoothing points) using the Unscrambler X 10.1 software (CAMO Software, Oslo, Norway) in order to normalize for the effects of differing sample thicknesses. The spectra from each group at the different ages were then analyzed using principal component analysis over spectral ranges of 1800-900 cm⁻¹ to distinguish the different biochemical components of each sample group.

Results

Histology of Subchondral Bone and Articular Cartilage from Normal and OA of the Knee

In the normal samples, histological staining revealed that the AC consisted of 3 areas - the superficial, transitional, and radial zones (Figure 1A(a)). The superficial zone

consisted of chondrocytes housed in lacunae. Mostly, each lacuna contained 1 cell. The transitional zone is located deep into the superficial zone. This zone contained spherical or ovoid-shaped chondrocytes. The radial zone contained chondrocytes that were arranged perpendicular to the articular surface. Some lacunae contained numbers of cells. This zone is located close to the calcified cartilage (CC)

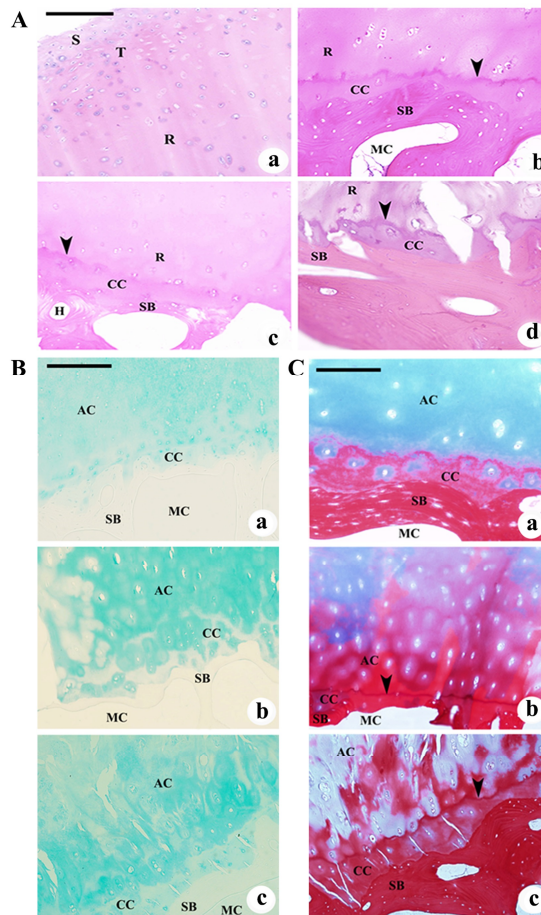


Figure 1. (A): Histology of condyles of the normal knee (a and b), young OA (c), and aged OA (d). The articular cartilage (AC) of the condyle is divided into the superficial zone (S), transitional zone (T), and radial zone (R). The radial zone is separated from the calcified cartilage (CC) by a tidemark (arrowhead). Deeper to the CC is the subchondral bone (SB). (B): Staining of proteoglycans in the condyles of the normal knee (a), young OA (b), and aged OA (c). (C): Staining of collagen fibers and bone matrix in the condyles of the normal knee (a), young OA (b), and aged OA (c). The collagen fibers are stained in blue and the bone matrix is stained in red. MC, medullary cavity. Scale bar = 200 μ m

and was separated from the CC by a tidemark (Figure 1A(b)). The CC lay close to the SB. The structures of the AC, CC, and SB of the young OA were seen similar to that of the normal person (Figure 1A(c)). In contrast, erosion was observed in the AC and CC of the aged OA (Figure 1A(d)).

Change of Proteoglycans of Subchondral Bone and Articular Cartilage from Normal and OA of the Knee

The normal samples contained proteoglycans that were distributed throughout the AC (Figure 1B(a)). Weaker staining of the proteoglycans was found in the CC. In the young OA, the strongest staining of the proteoglycans was observed in the AC and CC (Figure 1B(b)). The AC and CC of the aged OA showed weaker staining of the proteoglycans compared to those of the young OA (Figure. 1B(c)). However, the proteoglycans in the aged OA were stained stronger than that of the normal samples. No proteoglycans were stained in the SB of all the samples.

Change of Collagen Fibers of Subchondral Bone and Articular Cartilage from Normal and OA of the Knee

In the normal samples, collagen fibers were distributed homogeneously in the AC (Figure 1C(a)). No bone matrix was found in the AC. Collagen fibers were identified around the lacunae in the CC, but no collagen fibers were identified in the SB. The strongest staining of the bone matrix was observed in the SB.

In the young OA, the collagen fibers were observed only in the AC, and in weaker staining compared to that of the normal samples (Figure 1C(b)). No collagen fibers were found in the CC and SB. The matrix of the AC was partly replaced by the bone matrix. However, the staining of the bone matrix in the CC and SB were similar to those of the normal person. In the aged OA, the collagen fibers were not identified in all areas of the samples (Figure 1C(c)). In addition, the matrix of the AC was partly replaced by the bone matrix.

Changes of Biochemical of Subchondral Bone and Articular Cartilage from Normal

and OA People Investigated by Using SR-IR Microspectroscopy Technique

The use of the SR-IR microspectroscopy technique has been applied to determine the main component of the bone sample. The high resolution of the SR-IR technique can be used directly to measure each part of the samples: articulate cartilage, calcified cartilage, and subchondral bone (Kellgren and Lawrence, 2000; Knudson and Knudson, 2001; Kobrina *et al.*, 2012; Khanarian *et al.*, 2014; Kobrina, 2014). The infrared spectra of the samples with the different ages of the patients under OA conditions are shown in Figure 2. They are divided into 4 regions: (1) amide I collagen 1700-1600 cm^{-1} , (2) amide II collagen 1600-1500 cm^{-1} , (3) amide III collagen 1338 cm^{-1} , and (4) Proteoglycan carbohydrate 1140-985 cm^{-1} . Spectra features of IR spectra from the medial condyles specimens mainly originated from absorbance of the amide I, amide II, and amide III collagen molecules. Collagen molecules are the main component of cartilage's solid matrix which is strongly used for analysis of the collagen content. Amides II and III are related to CH₂ bending vibration, CH₃ asymmetric bending, and COO-stretching vibration. CH₂ side chain vibration of collagen, especially the small CH₂ side chain at 1340 cm^{-1} of the IR band, is usually important for the characterization feature of the collagen. The carbohydrate region (1140-980 cm^{-1}) is related to the stretching vibration of C-O, C-OH, and C-C ring vibration which is more specific to proteoglycans (Kobrina, 2014; Kumar *et al.*, 2015) which is another component of the extracellular matrix (Kellgren and Lawrence, 2000; Knudson and Knudson, 2001; Kobrina *et al.*, 2012; Khanarian *et al.*, 2014; Kobrina, 2014). The characteristic band assignment of bone samples can be classified into 4 regions as seen in Table 1.

Figure 4(a) shows the functional group area maps of a part of a tissue section from the articular cartilage (AC), calcified cartilage (CC), and subchondral bone (SB) achieved using SR-IR microspectroscopy point-to-point mapping with an aperture setting at 10×10 μm^2 . The average FTIR absorbance spectra of

the samples and the integral areas under OA conditions compared between the 3 areas of the normal and OA samples are shown in Figures 2(b)-2(d). The integrated peak areas of amide I (1700-1600 cm^{-1}), amide II (1600-1500 cm^{-1}), amide III (1338 cm^{-1}), and

proteoglycans (1140-985 cm^{-1}) were used and demonstrated on a histogram. The peak intensities of amide I significantly decreased in the AC of the young and aged OA (0.2073 ± 0.0019 and 0.2070 ± 0.0027 , respectively) compared to that of the normal samples

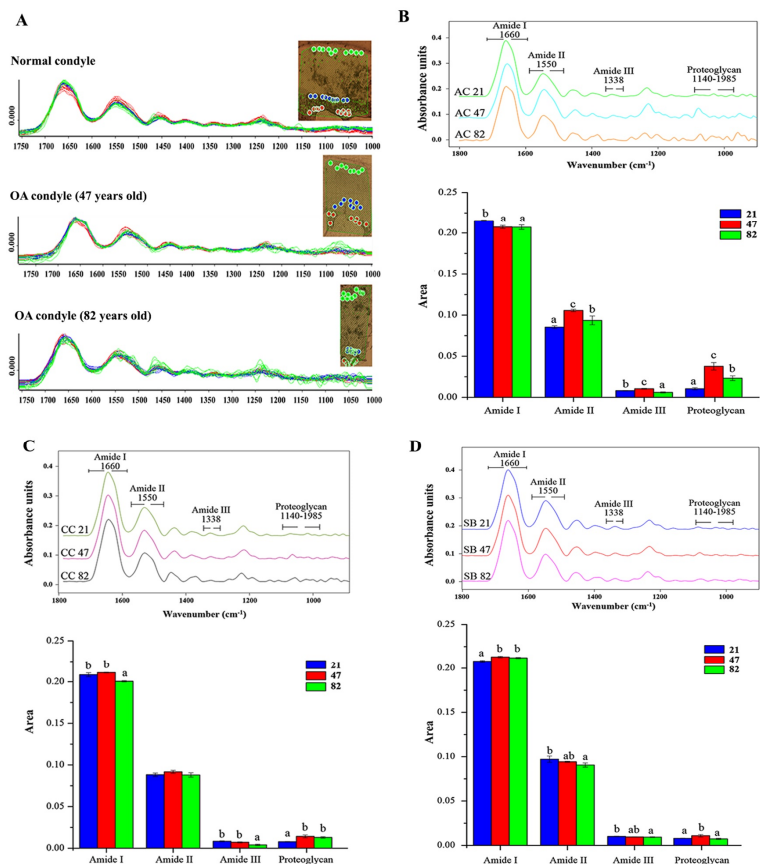


Figure 2. (A): Functional group area maps obtained under the spectral regions ranged from 1750-1000 cm^{-1} of the normal, young OA (47 years old), and aged OA (82 years old) at different area measurement: subchondral bone (red color), calcified cartilage (blue color), and articular cartilage (green color). The measurement was performed by point to point measurement with aperture setting at $10 \times 10 \mu\text{m}$ square aperture, 4 cm^{-1} 64 scans using SR-IR microspectroscopy. (B): Average original IR spectra extracted from the articular cartilage (AC) of the normal, young OA, and aged OA. (C): Average original IR spectra extracted from the calcified cartilage (CC) of the normal, young OA, and aged OA. (D): Average original IR spectra extracted from the subchondral bone (SB) of the normal, young OA, and aged OA. Approximately 100 spectra were collected from each group. Average spectra were preprocessed with 13 points of smoothing, baseline correction, and vector normalization over the spectral range of 1800-900 cm^{-1} . Different letters indicate significant differences

(0.2154 ± 0.0009) (Figure 2(b)). In contrast, the amide I peak intensities were significantly higher in the SB of both the young and aged OA (0.2133 ± 0.0008 and 0.2122 ± 0.0007 , respectively) compared to that of the normal samples (0.2084 ± 0.0009) (Figure 2(d)). The AC of the young OA showed the significant highest peak intensity of amide II (0.1057 ± 0.0013) (Figure 2(b)). The amide II significantly decreased in the aged OA (0.0936 ± 0.0054) compared to the young OA, but was still at a higher level than that of the normal samples (0.0854 ± 0.0016). There was no difference in the peak intensity of amide II in the CC of all samples (Figure 2(c)). However, in the SB of the aged OA, the amide II significantly decreased (0.0906 ± 0.0024), compared to that of the normal samples (0.0972 ± 0.0035) (Figure 2(d)).

Similar to the amide II, the peak intensity of amide III was significantly highest in the AC of the young OA (0.0104 ± 0.0005). However, the intensity was significantly lowest in the AC of the aged OA (0.0061 ± 0.0007) (Figure 2(b)). Moreover, the peak intensities of amide III in the CC and SB of the aged OA were significantly lower (0.0041 ± 0.0008 and 0.0093 ± 0.0004 , respectively) (Figure 2(c)-(d)) compared to those of the normal samples (0.0085 ± 0.0005 and 0.0101 ± 0.0003 , respectively). The degradation of

amide III and amide I was observed at the late stage of the OA samples, the same as the results compared with the spectra from the cartilage region. The degeneration of the AC and CC can be observed by these 2 bands. In the SB region, the increase of the amide I and the decrease of the amide II collagens was observed significantly at the late stage of OA persons. This biomarker band can be used to indicate orientation of the collagen fibril network (Kellgren and Lawrence, 2000; Knudson and Knudson, 2001; Kobrina *et al.*, 2012; Khanarian *et al.*, 2014; Kobrina, 2014; Kumar *et al.*, 2015).

The peak intensity of proteoglycans was significantly highest in the AC of the young OA (0.0377 ± 0.0045) (Figure 2(b)). The intensity decreased in the aged OA (0.0234 ± 0.0029), but was still at a higher level than that of the normal sample (0.0105 ± 0.0012). The SB of the aged OA contained a similar level of the proteoglycans to that of the normal sample (0.0073 ± 0.0007 and 0.0080 ± 0.0002 , respectively) (Figure 2(d)).

Integration Band Ratios of the Specimens

To demonstrate specifically the degrading of the collagen content, the integrated ratios of amide II/amide I, amide III/amide II, and proteoglycans/amide I can be used for quantification changes in the collagen network

Table 1. The Infrared absorption of the samples

Functional group	Wavenumber (cm ⁻¹)	References
1. Protein amide I collagen	1700-1600 cm ⁻¹	Kobrina <i>et al.</i> (2012);
Amide I C=O		Kobrina (2014)
Beta sheet	1638-1644 cm ⁻¹	
Alpha helix/Beta turn	1660-1668 cm ⁻¹	
Beta sheet	1692 cm ⁻¹	Figueiredo <i>et al.</i> (2012);
		Kobrina <i>et al.</i> (2012);
		Kobrina (2014)
2. Protein amide II (C-N stretching/NH bending/C-C stretching of collagens)	1600-1500 cm ⁻¹	
3. Protein amide III collagen	1338 cm ⁻¹	Boskey <i>et al.</i> (2007);
		Kobrina (2014)
4. Proteoglycan carbohydrate (C-O stretching vibration of carbohydrate residue in collagen and proteoglycans)	1140-985 cm ⁻¹	Potter <i>et al.</i> (2001); Kobrina (2014)

during the OA progression (Kellgren and Lawrence, 2000; Knudson and Knudson, 2001; Kobrina *et al.*, 2012; Khanarian *et al.*, 2014; Kobrina, 2014; Kumar *et al.*, 2015).

In the AC, the amide II/amide I ratio significantly increased in both the young and aged OA (0.5098 ± 0.0096 and 0.4522 ± 0.0291) compared to that of the normal sample (0.3962 ± 0.0058) (Figure 3(a)). This ratio was at a similar level in the CC of all the samples (0.4233 ± 0.0138 , 0.4348 ± 0.0069 , and 0.4388 ± 0.0144 in the normal, young OA, and aged OA, respectively) (Figure 3(b)). In contrast, the ratio significantly decreased in the SB of the aged OA (0.4271 ± 0.0122) compared to the

normal sample (0.4663 ± 0.0177) (Figure 3(c)). The amide III/amide II ratio was significantly lowest in the AC and CC of the aged OA (0.0648 ± 0.0037 and 0.0465 ± 0.0088 , respectively) (Figure 3(a-b)). Those ratios of the normal samples were 0.0961 ± 0.0034 and 0.0958 ± 0.0047 , respectively. However, no significant difference of the ratio was observed in the SB of all the samples (0.1040 ± 0.0047 , 0.1008 ± 0.0016 , and 0.1032 ± 0.0036) in the normal, young OA, and aged OA, respectively (Figure 3(c)). The proteoglycans/amide I ratio was significantly highest in the AC of the young OA (0.1821 ± 0.0230) (Figure 3(a)). The AC of the aged OA showed a decrease in the

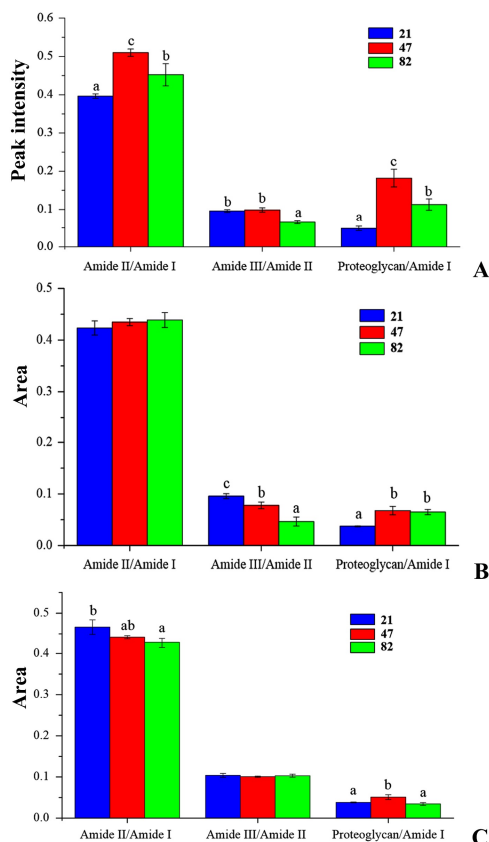


Figure 3. The integrated ratio of the peak intensities of IR spectra extracted from the articular cartilage (A), calcified cartilage (B), and subchondral bone (C) of the normal condyle and the young and aged OA. Average spectra were preprocessed with 13 points of smoothing, baseline correction, and vector normalization over the spectral range of $1800\text{-}900\text{ cm}^{-1}$. Different letters indicate significant differences

proteoglycans/amide I ratio (0.1129 ± 0.0147) compared to that of the young OA. However, this ratio was still higher compared to that of the normal samples (0.0486 ± 0.0058). The proteoglycans/amide I ratio was significantly higher in the CC of both the young and aged OA (0.0678 ± 0.0081 and 0.0649 ± 0.0050 , respectively), compared to those of the normal samples (0.0374 ± 0.0010) (Figure 3(b)). However, in the SB, this ratio for the aged OA was at a similar level compared to that of the normal samples (0.0345 ± 0.0034 and 0.0383 ± 0.0010 , respectively) (Figure 3(c)).

The Overall Integral Areas of the Amide Collagen of the Specimens

The sum of the spectra of amide I ($1700-1600 \text{ cm}^{-1}$), amide II ($1600-1500 \text{ cm}^{-1}$), and amide III (1338 cm^{-1}) are shown in Table 2.

In the AC and CC, it appeared that the significantly highest level of the sum of the amides was observed in the young OA (0.323 ± 0.001 and 0.310 ± 0.002 , respectively). The AC and CC of the aged OA showed lower levels of the sum of the amides (0.307 ± 0.005 and 0.293 ± 0.002 , respectively) compared to that of the normal samples (0.309 ± 0.003 and 0.305 ± 0.001 , respectively) in which a significant difference was observed in the CC. The SB of the normal and both the young and aged OA showed no significant difference in the sum of the Amides (0.316 ± 0.003 , 0.317 ± 0.001 , and 0.312 ± 0.002 , respectively).

Principal Component Analysis

Principal component analysis (PCA) is a statistical data-reduction method which transforms the original data set of variables into a new set of uncorrected variables known as principal

components (PCs). The PCA was performed on the original spectra acquired from the articular cartilage, calcified cartilage, and subchondral bone. The output of the data analysis can be presented either as 2 dimensional (2 PCs) or in 3-D using 3 PCs. The use of multivariate analysis, in particular PCA, has proven to be useful in the analysis of biospectroscopic data by providing 2 types of information: visualization of clustering of similar spectra within datasets in scores plots; and identification of variables (spectral bands representing various molecular groups within the samples) in loadings plots explaining the clustering observed in the scores plots (Matsui *et al.*, 1997; Kobrina, 2014).

The PCA analysis of all areas of the samples is shown in Figure 4. The PCA score plot showed that spectra from the 3 areas were clustered separately along PC1, PC2, and PC3. The positive loading was plotted from the PC1 loading at 1629 cm^{-1} , 1538 cm^{-1} , 1201 cm^{-1} , 1076 cm^{-1} , and 958 cm^{-1} in the positive-score plot of the AC spectra of the young and aged OA. The negative was plotted from the PC3 loading at 1679 cm^{-1} , 1550 cm^{-1} , 1450 cm^{-1} , and 1332 cm^{-1} which explained the cluster between areas. From the PCA analysis, it was shown that the main spectra changes contributed to spectra from the cartilage of the aged OA. The spectra change in terms of the amide I alpha helix structure (1660 cm^{-1}) was shifted to the amide I beta sheet structure (1631 cm^{-1}) when compared with the normal samples. The spectra from the normal samples were clearly observed in the negative PC3 score plot corresponding with the negative PC3 loading at 1646 cm^{-1} , 1589 cm^{-1} , 1137 cm^{-1} , and 979 cm^{-1} . The spectra from the SB were observed

Table 2. The sum of integral areas of amides I, II, and III obtained from spectra of the articular cartilage, calcified cartilage, and subchondral bone

Component	Integral area		
	21 years old normal	47 years old OA	82 years old OA
Articular cartilage	0.309 ± 0.003^a	0.323 ± 0.001^b	0.307 ± 0.005^a
Calcified cartilage	0.305 ± 0.001^b	0.310 ± 0.002^c	0.293 ± 0.002^a
Subchondral bone	0.316 ± 0.003	0.317 ± 0.001	0.312 ± 0.002

Note: Different superscript letters in the same row indicate significant differences ($P < 0.05$, Duncan's new multiple range test)

in the spectral changes in amide I and II which could imply the change in collagen orientation. Osteoarthritis and degeneration of the articular cartilage were involved in the change in orientation of the collagen fibril network. The structural changes in terms of the amide I alpha helix and amide I beta sheet are important points that are involved in the spectral changes in the cartilage at the late stage of age (Kobrina *et al.*, 2012; Kobrina, 2014).

Discussion

Infrared analysis of bone and cartilage has proven to be a valuable technique in the field

of OA. It is a powerful tool for establishing the important material properties' contribution to better understand the changes in fragile bone and cartilage. Synchrotron-based FTIR microspectroscopy has introduced a novel method to study the chemical composition distribution of biological components which can be applied to obtain results with high spatial resolution. The FTIR technique is an alternative choice to gain information from the collagens (amides I, II, and III) represented from the peptide bond C = O stretching, C-N stretching, and N-H bending (Guilak *et al.*, 1994; Knudson and Knudson, 2001; Kobrina *et al.*, 2012; Khanarian *et al.*, 2014).

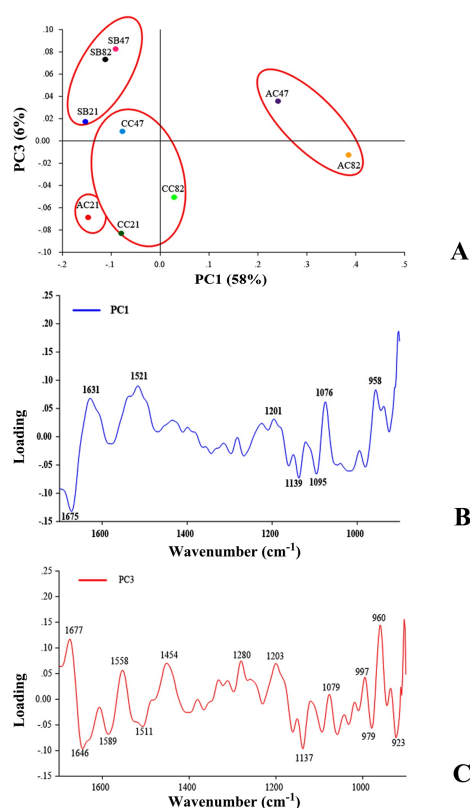


Figure 4. The PCA score plot (A), the loading PC1 (B), and PC3 (C) of IR spectra from different regions of the samples: articular (AC), calcified cartilage (CC), and subchondral bone (SB) of the 21 years old normal person and OA people (47 and 82 years old). Averages of the spectra were preprocessed with 13 points of smoothing, baseline correction, and vector normalization over the spectral ranges of 1800-900 cm^{-1}

In the present study, histochemical staining of the proteoglycans showed that amount of proteoglycans in the AC of the young OA increased when compared to that of the normal samples. The proteoglycans were decreased in the aged OA, but was still stronger than that of the normal condyle. This was similar to the result obtained from the SR-IR microspectroscopy and those of previous investigations. A study reported that the rate of proteoglycan synthesis increased in the early OA condition (Knudson and Knudson, 2001). This could be related to a repairing process of the cartilage. The rate of proteoglycan synthesis decreased with the progression of OA which caused an elevation in the apoptotic rate of the chondrocytes (Nelson *et al.*, 2006). Thus, the amount of the proteoglycans decreased in the late stage of OA (Muller-Gerbl *et al.*, 1989; Nelson *et al.*, 2006; Oinas *et al.*, 2016). Various studies using humans as models revealed that a decrease in proteoglycans was obviously observed only in the advanced stage of OA (Hattori *et al.*, 2007). In the advanced stage of OA, the loss of proteoglycans in the AC is considered to be a hallmark of the osteoarthritic process (Takahashi *et al.*, 2014). It was found that, after any injury, hyaline cartilages were replaced by fibrocartilage which contained predominantly collagen type I and low amounts of proteoglycans (Radin *et al.*, 1970; Muller-Gerbl *et al.*, 1989; Matsui *et al.*, 1997; Panula *et al.*, 1998; Price *et al.*, 2002; Nelson *et al.*, 2006; Oinas *et al.*, 2016). Histochemical staining was not able to detect the proteoglycans in the SB of all the people, whereas the SR-IR microspectroscopy showed the ability to do so. This suggests that the FTIR achieves molecular information at a higher spatial resolution than that of the histochemical staining. Thus, SR-IR microspectroscopy could overcome the limitation of histochemical staining in detection of biochemical changes in the samples of OA.

Histochemical staining showed a decrease in the amounts of collagens in the OA knee, especially that of the aged OA. This is in agreement with results reported in previous studies (Eckstein *et al.*, 1992; Eckstein *et al.*, 1995). It was found that the AC of OA

knees degenerated in association with the denaturation of type II collagens (Dragica *et al.*, 2003). Some studies reported that OA knees had an increase in the percent denaturation of the type II collagens which were found to be cleaved by collagenases (Stoop *et al.*, 2001). Some research (Radin *et al.*, 1970; Muller-Gerbl *et al.*, 1989; Rizkalla *et al.*, 1992; Matsui *et al.*, 1997; Panula *et al.*, 1998; Price *et al.*, 2002; Saarakkala *et al.*, 2003; Lajeunesse 2004; Nelson *et al.*, 2006; Saarakkala *et al.*, 2010; Kobrina *et al.*, 2012; Rieppo *et al.*, 2012; Kobrina 2014; Kumar *et al.*, 2015; Oinas *et al.*, 2016) stated that the degradation of amides I and III was observed at the late stage of age. However, the SR-IR microspectroscopy revealed more details. This technique showed that the level of the sum of amides was significantly highest in the AC and CC of the young OA. In contrast, all parts of the samples of the aged OA showed lower levels of the sum of amides compared to that of the normal samples in which a significant difference was observed in the CC.

In OA, the degradation of the extracellular matrix of the AC may occur and its function may be inhibited. Degenerative changes include the disruption of collagen fibrils that restricts the proteoglycan-water binding capacity and leads to swelling. The changes in collagen and proteoglycans contents play an important factor in disease progression. During the progression of OA, the associated changing in the molecular composition and organization of the cartilage matrix leads to deterioration in the material properties and structural integrity of the articular surface (Goldring and Goldring, 2010). One of many signs of early OA is the decreasing in proteoglycans from the cartilage surface and fibrillation of the superficial collagen network (Sabatini *et al.*, 2000; Schmitz *et al.*, 2010; Schneevoigt *et al.*, 2017). After this change, cartilage tissue begins to swell and its water content increases. Consequently, the mechanical property of AC deteriorates. Especially, dynamic stiffness of the tissue decreases in the early stage of OA (Hada *et al.*, 2014). Characterization of these changes is crucial if one wants to understand the processes of OA.

Spectral analysis using confocal Raman spectroscopy indicated that the content of disordered coil collagen increased significantly during the early progression of OA (Takahashi *et al.*, 2014). In the present study, the amounts of amide III in the AC of the young OA increased when compared to that of the normal samples. It was indicated that the higher intensity of amide III revealed the higher content of disordered collagen. This could be used as evidence for defective collagen leading to the abnormality of the cartilage structure (Hattori *et al.*, 2007). After a defect of the cartilage, regenerative tissue showed significant changes in collagen distribution compared to normal cartilage with collagen fibrils demonstrating a random orientation. Loss in proteoglycan content was also shown (Rieppo *et al.*, 2012).

From the overall results, it can be concluded that articular cartilage is mainly distributed to OA progression in the late stage of the OA samples (47 years and 82 years) as observed in the increase in the amide II/amide I ratio, amide III/amide I ratio, and proteoglycans/amide I when compared with the normal samples. The amide II/amide I ratio was observed to be significantly higher in the AC of both the young and aged OA compared to that of the normal samples. The ratio of amide II/amide I was utilized as a spectral marker of collagen orientation. Since the amide I and amide II vibration modes have transition vibration indicating the transition moment's approximately perpendicular directions, it can be implied that there is degradation of the collagen network (Knudson and Knudson, 2001; Stoop *et al.*, 2001; Kobrina *et al.*, 2012; Khanarian *et al.*, 2014). This result suggests that the change in the chemical compositions of the AC is caused by the progression of OA. SR-IR microspectroscopy can be rapidly applied to characterize the distribution and structure of the articular cartilage components. It also can provide valuable information in revealing compositional and structural changes in the articular cartilage which is an indicator to detect the early stage of OA.

Conclusions

In summary, it can be concluded that the cartilage of the medial femoral condyles was the main structure that was affected by the progression of OA caused by the decrease in the level of the sum of the amides. OA also was involved in the change in orientation of the collagen fibrils network and structural changes in terms of the amide I alpha helix and amide I beta sheet. This study demonstrated that SR-IR microspectroscopy can be rapidly applied to characterize the distribution and structure of cartilage components. It also enables the correlation between cartilage properties and function. Moreover, SR-IR microspectroscopy can provide valuable information to reveal compositional and structural changes in cartilage which is an indicator for the detection of the early stage of osteoarthritic degradation. This work helps us to better understand OA.

Acknowledgements

This paper is a cooperation between SLRI, and the School of Preclinic, Institute of Science and the Medical Faculty, Institute of Medicine, Suranaree University of Technology. Many thanks to beam line 4.1: Infrared Spectroscopy and Imaging and Suranaree University of Technology Hospital for kindly providing facilities.

References

- Aigner, T., Fundel, K., Saas, J., Gebhard, P.M., Haag, J., Weiss, T., Zien, A., Obermayr, F., Zimmer, R., and Bartnik, E. (2006). Large-scale gene expression profiling reveals major pathogenetic pathways of cartilage degeneration in osteoarthritis. *Arthritis Rheum.*, 54(11):3533-3544.
- Bobinac, D., Spanjol, J., and Zoricic, S. (2003). Changes in articular cartilage and subchondral bone histomorphometry in osteoarthritic knee joints in humans. *Bone*, 32(3):284-290.
- Boskey, A. and Camacho, N.P. (2007). FT-IR imaging of native and tissue-engineered bone and cartilage. *Biomaterials*, 28(15):2465-2478.
- Chappard, C., Peyrin, F., Bonnassie, A., Lemineur, G.,

- Brunet-Imbault, B., Lespessailles, E., and Benhamou, C.L. (2006). Subchondral bone micro-architectural alterations in osteoarthritis: a synchrotron micro-computed tomography study. *Osteoarthr. Cartilage*, 14(3):215-223.
- Dragica, B., Josip, S., Sanja, Z., and Ivana, M. (2003). Changes in articular cartilage and subchondral bone histomorphometry in osteoarthritic knee joints in humans. *Bone*, 32:284-290.
- Eckstein, F., Milz, S., Anetzberg, H., and Putz, R. (1998). Thickness of the subchondral mineralized tissue zone (SMZ) in normal male and female and pathological human patellae. *J. Anat.*, 192:81-90.
- Eckstein, F., Muller-Gerbl, M., Steinlechner, M., Kierse, R., and Putz, R. (1995). Subchondral bone density of the human elbow assessed by computed tomography osteoabsorptiometry: a reflection of the loading history of the joint surfaces. *J. Orthop. Res.*, 13(2):268-278.
- Eckstein, F., Muller-Gerbl, M., and Putz, R. (1992). Distribution of subchondral bone density and cartilage thickness in the human patella. *J. Anat.*, 180:425-433.
- Figueiredo, M.M., Gamelas, J.A.F., and Martins, A.G. (2012). Characterization of bone and bone-based graft materials using FTIR spectroscopy. In: *Infrared Spectroscopy - Life and Biomedical Sciences*. Theophile, T. (ed). In Tech, London, UK, p. 315-338.
- Goldring, M.B., and Goldring, S.R. (2010). Articular cartilage and subchondral bone in the pathogenesis of osteoarthritis. *Ann. NY Acad. Sci.*, 1192:230-237.
- Guilak, F., Ratcliffe, A., Lane, N., Rosenwasser, M.P., and Mow, V.C. (1994). Mechanical and biochemical changes in the superficial zone of articular cartilage in canine experimental osteoarthritis. *J. Orthop. Res.*, 12:474-484.
- Hada, S., Kaneko, H., Sadatsuki, R., Liu, L., Futami, I., Kinoshita, M., Yusup, A., Saita, Y., Takazawa, Y., Ikeda, H., Kaneko, K., and Ishijima, M. (2014). The degeneration and destruction of femoral articular cartilage shows a greater degree of deterioration than that of the tibial and patellar articular cartilage in early stage knee osteoarthritis: a cross-sectional study. *Osteoarthr. Cartilage*, 22(10):1583-1589.
- Hattori, S., Sakane, M., Mutsuzaki, H., Tanaka, J., Ochiai, N., and Nakajima, H. (2007). Chondrocyte apoptosis and decrease of glycosaminoglycan in cranial cruciate ligament insertion after resection in rabbits. *J. Vet. Med. Sci.*, 69(3):253-258.
- Ijiri, K., Zerbini, L.F., Peng, H., Otu, H.H., Tsuchimochi, K., Otero, M., Dragomir, C., Walsh, N., Bierbaum, B.E., Mattingly, D., van Landern, G., Komiya, S., Aigner, T., Libermann, T.A., and Goldring, M.B. (2008). Differential expression of GADD45 in normal and osteoarthritic cartilage: potential role in homeostasis of articular chondrocytes. *Arthritis Rheum.*, 58(7):2075-2087.
- Kamibayashi, L., Wyss, U.P., Cooke, T.D.V., and Zec, B. (1995). Trabecular microstructure in the medial condyle of the proximal tibia of patients with knee osteoarthritis. *Bone*, 17:27-35.
- Kellgren, J.H. and Lawrence, J.S. (2000). Radiological assessment of osteo-arthrosis. *Ann. Rheum. Dis.*, 16(4):494-502.
- Khanarian, N.T., Boushell, M.K., Spalazzi, J.P., Pleshko, N., Boskey, A.L., Lu, H.H. (2014). FITI-I compositional mapping of the cartilage to bone interface as a function of tissue region and age. *J. Bone Miner. Res.*, 29(12):2643-2652.
- Knudson, C.B. and Knudson, W. (2001). Cartilage proteoglycans. *Semin. Cell Dev. Biol.*, 12:69-78.
- Kobrina, Y., Rieppo, L., Saarakkala, S., Jurvelin, J.S., and Isaksson, H. (2012). Clustering of infrared spectra reveals histological zones in intact articular cartilage. *Osteoarthr. Cartilage*, 20(5):460-468.
- Kobrina, Y. (2014). *Infrared Microspectroscopic Cluster Analysis of Bone and Cartilage*. Dissertation in Forestry and Natural Sciences, The University of Eastern Finland, Kuopio, Finland, 103p.
- Kumar, R., Gronhaug, K.M., Afseth, N.K., Isaksen, V., de Lange Davies, C., Drogset, J.O., and Lilledahl, M.B. (2015). Optical investigation of osteoarthritis human cartilage (ICRS grade) by confocal Raman spectroscopy: a pilot study. *Anal. Bioanal. Chem.*, 407:8067-8077.
- Lajeunesse, D. (2004). The role of bone in the treatment of osteoarthritis. *Osteoarthr. Cartilage*, 12(Supplement A):S34-S38.
- Matsui, H., Shimizu, M., and Tsuji, H. (1997). Cartilage and subchondral bone interaction in osteoarthritis of human knee joint: a histological and histomorphometric study. *Microsc. Res. Techniq.*, 37(4):333-342.
- Muller-Gerbl, M., Putz, R., Hodapp, N., Schulte, E., and Wimmer, B. (1989). Computed tomography-osteabsorptiometry for assessing the density distribution of subchondral bone as a measure of long term mechanical adaptation in individual joints. *Skeletal Radiol.*, 18(7):507-512.
- Nelson, F., Billingham, R.C., Pidoux, I., Reiner, A., Langworthy, M., McDermott, M., Malogne, T., Sitler, D.F., Kilambi, N.R., Lenczner, E., and Poole, A.R. (2006). Early post-traumatic osteoarthritis-like changes in human articular cartilage following rupture of the anterior cruciate ligament. *Osteoarthr. Cartilage.*, 14:114-119.
- Oinas, J., Rieppo, L., Finnilä, M.A.J., Valkealahti, M., Lehenkari, P., and Saarakkala, S. (2016). Imaging of osteoarthritic human articular cartilage using Fourier transform infrared microspectroscopy combined with multivariate and univariate analysis. *Sci. Rep-UK*, 6:30008.
- Panula, H.E., Hyttinen, M.M., Arokoski, J.P., Langsjo, T.K., Peltari, A., Kiviranta, I., and Helminen, H.J. (1998). Articular cartilage superficial zone collagen birefringence reduced and cartilage thickness increased before surface fibrillation in experimental osteoarthritis. *Ann. Rheum. Dis.*, 57:237-245.
- Potter K, Kidder LH, Levin IW, Lewis EN, Spencer RG. (2001). Imaging of collagen and proteoglycan in cartilage sections using Fourier transform infrared. *Arthritis Rheum.*, 44(4):846-855.
- Price, J.S., Chambers, M.G., Poole, A.R., Fradin, A., and Mason, R.M. (2002). Comparison of collagenase-

- cleaved articular cartilage collagen in mice in the naturally occurring STR/ort model of osteoarthritis and in collagen-induced arthritis. *Osteoarthr. Cartilage*, 10:172-179.
- Radin, E.L., Paul, I.L., and Tolkoff, M.J. (1970). Subchondral bone changes in patients with early degenerative joint disease. *Arthritis Rheum.*, 13:400-405.
- Rieppo, L., Rieppo, J., Jurvelin, J.S., and Saarakkala, S. (2012). Fourier transform infrared spectroscopic imaging and multivariate regression for prediction of proteoglycan content of articular cartilage. *Plos One*, 7(2):1-8.
- Rizkalla, G., Reiner, A., Bogoch, E., and Poole, A.R. (1992). Studies of the articular cartilage proteoglycan aggrecan in health and osteoarthritis. *J. Clin. Invest.*, 90:2268-2277.
- Saarakkala, S., Laasanen, M.S., Jurvelin, J.S., Torronen, K., Lammi, M.J., Lappalainen, R., and Toyras, J. (2003). Ultrasound indentation of normal and spontaneously degenerated bovine articular cartilage. *Osteoarthr. Cartilage*, 11(9):697-705.
- Saarakkala, S., Rieppo, L., Rieppo, J., and Jurvelin, J.S. (2010). Fourier transform infrared (FTIR) microspectroscopy of immature, mature and degenerated articular cartilage. In: *Microscopy: Science, Technology, Applications and Education*. Méndez-Vilas, A. and Díaz, J. (eds). Formatex Research Center, Badajoz, Spain, p. 403-414.
- Sabatini, M., Rolland, G., Léonce, S., Thomas, M., Lesur, C., Pérez, V., de Nanteuil, G., and Bonnet, J. (2000). Effects of ceramide on apoptosis, proteoglycan degradation, and matrix metalloproteinase expression in rabbit articular cartilage. *Biochem. Biophys. Res. Co.*, 267:438-444.
- Schmitz, N., Laverty, S., Kraus, V.B., and Aigner, T. (2010). Basic methods in histopathology of joint tissues. *Osteoarthr. Cartilage*, 18:S113-116.
- Schneevoigt, J., Fabian, C., Leovsky, C., Seeger, J., and Bahramsoltani, M. (2017). In vitro expression of the extracellular matrix components aggrecan, collagen type I and II by articular cartilage-derived chondrocytes. *Anat. Histol. Embryol.*, 46(1):43-50.
- Sindhupakorn, B., Thienpratharn, S., and Kidkhunthod, P. (2017). A structural study of bone changes in knee osteoarthritis by synchrotron-based X-ray fluorescence and X-ray absorption spectroscopy techniques. *J. Mol. Struct.*, 1,146:254-258.
- Stoop, R., Buma, P., van der Kraan, P.M., Hollander, A.P., Billinghamurst, R.C., Meijers, T.H., Poole, A.R., and van den Berg, W.B. (2001). Type II collagen degradation in articular cartilage fibrillation after anterior cruciate ligament transection in rats. *Osteoarthr. Cartilage*, 9:308-315.
- Takahashi, Y., Sugano, N., Takao, M., Sakai, T., Nishii, T., and Pezzotti, G. (2014). Raman spectroscopy investigation of load-assisted microstructural alterations in human knee cartilage: preliminary study into diagnostic potential for osteoarthritis. *J. Mech. Behav. Biomed.*, 31:77-85.
- Temple, M.M., Bae, W.C., Chen, M.Q., Lotz, M., Amiel, D., Coutts, R.D., and Sah, R.L. (2007). Age- and site-associated biomechanical weakening of human articular cartilage of the femoral condyle. *Osteoarthr. Cartilage*, 15(9):1042-1052.